Design and Tests of an Adaptive Triggering Method for Capturing Peak Samples in a Thin Phytoplankton Layer by an Autonomous Underwater Vehicle

Yanwu Zhang, *Senior Member, IEEE*, Robert S. McEwen, *Member, IEEE*, John P. Ryan, and James G. Bellingham

***Abstract*—Thin layers of phytoplankton have an important impact on coastal ocean ecology. The high spatial and temporal variability of such layers makes autonomous underwater vehicles (AUVs) ideal for their study. At the Monterey Bay Aquarium Research Institute (MBARI, Moss Landing, CA), the authors have used an AUV for obtaining repeated high-resolution surveys of thin layers in Monterey Bay, CA. The AUV is equipped with ten "gulpers" that can capture water samples when some feature is detected. In this paper, the authors present an adaptive triggering method for an AUV to capture water samples at chlorophyll fluorescence peaks in a thin layer. The algorithm keeps track of the fluorescence background level and the peaks' baseline in real time to ensure that detection is tuned to the ambient conditions. The algorithm crosschecks for concurrent high values of optical backscattering to ensure that sampling targets true particle peaks and not simply physiologically controlled fluorescence peaks. To let the AUV capture the thin layer's peak without delay, the algorithm takes advantage of the vehicle's sawtooth (i.e., yo-yo) trajectory: in one yo-yo cycle, the vehicle makes two crossings of the thin layer. On the first crossing, the vehicle detects the layer's fluorescence peak and saves the peak height; on the second crossing, as the fluorescence measurement reaches the saved peak height (plus meeting additional timing and depth conditions), a sampling is triggered. Based on the thin layer's vertical position in the vehicle's yo-yo profiles, the algorithm selects the pair of detection and triggering crossings so as to minimize the spacing between them. We use the algorithm to postprocess a data set of 20 AUV missions in the 2005 Layered Organization in the Coastal Ocean (LOCO) Experiment in Monterey Bay, CA, and compare its performance with that of a threshold triggering method. In October 2009, the presented method was field tested in an AUV mission in northern Monterey Bay, CA.**

***Index Terms*—Autonomous underwater vehicle (AUV), peak detection, thin phytoplankton layer, water sample acquisition.**

I. Introduction

THIN layers of phytoplankton are often observed in the coastal ocean [1]–[5]. They have an important impact on the patterns of primary productivity, the survival and growth of zooplankton and fish larvae, the development of harmful algal blooms (HABs), and other aspects of coastal ocean ecology [1]–[5]. Thin layers have a thickness ranging from <1 m to a few meters, and can horizontally extend for kilometers [1], [3]–[5]. For studying thin layers, high-resolution sampling in the vertical dimension is required.

Fig. 1. The ten gulpers on the Dorado AUV (courtesy of L. Bird and A. Sherman of MBARI).

At the Monterey Bay Aquarium Research Institute (MBARI, Moss Landing, CA), we operate a Dorado AUV [6], [7] to conduct surveys for interdisciplinary oceanographic studies. The vehicle has a length of 4.2 m and a diameter of 0.53 m at the midsection. Its sensor suite includes Sea-Bird SBE3 temperature and SBE4 conductivity sensors, a Paroscientific 8CB4000-I pressure sensor, and a HOBI Labs HydroScat-2 sensor that measures chlorophyll fluorescence at the 676-nm wavelength and backscatter at two wavelengths (470 and 676 nm before February 2009, and 420 and 700 nm afterwards). While *in situ* measurements are essential for an AUV survey, many important chemical and biological properties of seawater can only be measured in the laboratory, which calls for collecting water samples and returning them to shore. AUV-borne water samplers are particularly needed for the studies of plankton and larval ecology, primary production, and HABs [8]. MBARI engineers designed and installed ten 2-L "gulpers" [9] on a Dorado AUV, as shown in Fig. 1, which can capture water samples when some feature is detected.

Manuscript received February 23, 2010; revised July 07, 2010; accepted September 17, 2010. Date of publication October 21, 2010; date of current version November 30, 2010. This work was supported by the David and Lucile Packard Foundation.

Associate Editor: H. Singh.

The authors are with the Monterey Bay Aquarium Research Institute, Moss Landing, CA 95039 USA (e-mail: yzhang@mbari.org; rob@mbari.org; ryjo@mbari.org; jgb@mbari.org).

Digital Object Identifier 10.1109/JOE.2010.2081031

Within a thin layer, a high biomass concentration leads to a high level of chlorophyll fluorescence [5]. Therefore, for investigating the peak biomass, it is a critical task to have the gulpers capture water samples at fluorescence peaks. As a first step, the second and third authors devised a threshold triggering method for capturing high-fluorescence water samples as follows.

1) Based on premission field measurements of fluorescence (such as in a preceding AUV mission), set an appropriate fluorescence threshold $\mathrm{FL}_{\mathrm{thresh}}$.
2) During the mission, when J out of K past (including the current) fluorescence measurements [i.e., samples $n, n-1, \ldots, n-(K-1)$] exceed $\mathrm{FL}_{\mathrm{thresh}}$, consider the threshold met. This "J out of K" (e.g., 4 out of 8) condition is for rejecting noise spikes and outliers.
3) Set a lockout time interval T_{lockout} between triggerings to prevent "dense triggerings" that would use up gulpers over a short distance. A triggering is allowed only if the elapsed time since the last triggering exceeds T_{lockout}.
4) To prevent gulping air bubbles, a triggering is allowed only if the vehicle's depth exceeds a lockout depth $\mathrm{DEP}_{\mathrm{lockout}}$.

As will be demonstrated in the field test results in Section IV, the threshold triggering method is a practical and robust mechanism for capturing high-fluorescence water samples. However, this method has two shortcomings. 1) A fluorescence threshold needs to be set prior to the mission. If the threshold is set too low, the water sample acquisition capacity will be expended too rapidly. As a result, some truly high-chlorophyll patches will be missed. If the threshold is set too high, triggerings will be scarce, so the water sample acquisition capacity will be underutilized. 2) A sampling is triggered as soon as the threshold condition is met, without the capacity of "waiting for" an ensuing peak. On the basis of the threshold triggering method and to overcome its shortcomings, we have developed an adaptive peak-detection triggering method [10].

Real-time peak detection is a difficult problem. The basic approach of gradient (i.e., slope) tracking—declaring a peak when the sign of the slope flips from positive to negative [11]—works well in postprocessing, but not in real time: when it is found that the gradient has just turned negative, the peak has already passed. As a result, peak detection would come late. To prevent false peak detections caused by noise spikes or minor bumps, lowpass filtering is commonly required, which adds an additional delay in peak detection.

An example of peak detection is illustrated in Fig. 2. On the raw measurement (the solid line), the peak lies at time index n, but the flipping of the slope's sign can only be detected at $n+1$. Hence, the peak detection on the solid line comes at $n+1$, late by one sample. Note that the raw measurement has two minor peaks at $n-2$ and $n+2$. To remove those two minor peaks, we lowpass filter the raw measurement by a two-sample moving-average window, resulting in the dashed line. This lowpass filtering carries a delay of one sample, hence "moving" the peak from n to $n+1$. Consequently, peak detection by gradient tracking on the dashed line comes at $n+2$. Thus, the total delay in peak detection is now two samples. In practice, more intense lowpass filtering is often required to suppress stronger noise, which means an even longer delay. For instance, a seven-sample moving-average window will cause a delay of $(7-1)/2 = 3$ samples. Then, the total delay in peak detection will be $1+3 = 4$ samples. The sampling interval of the HydroScat-2 fluorescence and backscatter sensor is 0.25 s. So a four-sample delay means a delay of 1 s. If an AUV carrying a HydroScat-2 sensor crosses a thin layer of a 0.5-m thickness at a vertical speed of 0.5 m/s, a 1-s delay means that the AUV will miss the layer.

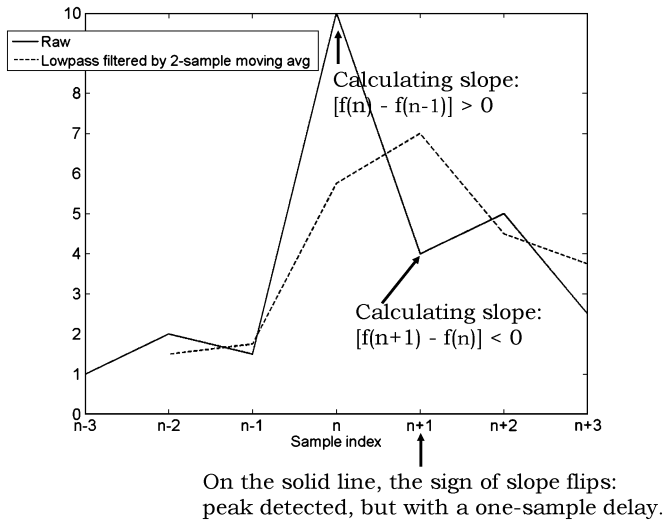

Fig. 2. If using slope tracking for real-time peak detection, the detection would come late.

Another type of approach, under the premise that the signal shape is known *a priori*, employs the technique of matched filtering [12] for peak detection [13], [14]. However, not only is the computation more complicated, but also the variability of oceanographic signals often makes it infeasible to assume a signal shape *a priori*.

In our adaptive peak-detection triggering method, we enable an AUV to capture peaks without delay by taking advantage of the vehicle's sawtooth (i.e., yo-yo) trajectory. There is no need to preset a triggering threshold. Rather, the vehicle automatically determines whether a detected peak qualifies as a "high peak" for triggering. The method is presented in Section II. To evaluate the statistical performance, we use the algorithm to postprocess a previous AUV data set, as discussed in Section III. The method was field tested in an AUV mission in northern Monterey Bay, CA, in October 2009. The results are presented in Section IV. We give the conclusion and propose future work in Section V. Note that the presented method is for capturing water samples in a horizontal thin layer where the signal reaches a peak at some depth (i.e., in the vertical dimension). There are a variety of other oceanographic processes, such as a front between different water masses, that exhibit signal peaks (or peaks of the signal's gradient) in the horizontal dimension. We are working to extend our method to capturing peaks in the horizontal dimension.

II. An Adaptive Triggering Method Based on Real-Time Peak Detection

In a thin phytoplankton layer, chlorophyll fluorescence and backscatter intensities exceed background levels [2]. When an AUV traverses the layer, it can detect a fluorescence peak. As

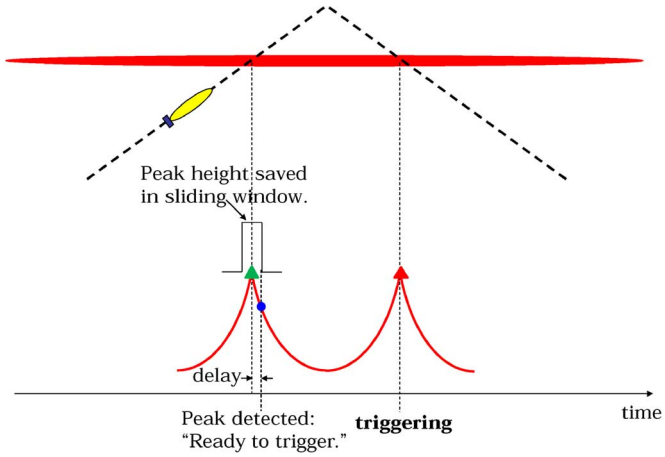

Fig. 3. On its sawtooth trajectory through a thin phytoplankton layer, an AUV detects the fluorescence peak on the first crossing, with a delay. It captures the peak on the second crossing with no delay.

discussed in Section I, peak detection cannot escape a delay in a single crossing of the layer. However, in an ascent–descent cycle (i.e., a sawtooth cycle), the AUV makes two crossings of the layer, as illustrated in Fig. 3. The crux of our method is to overcome the peak-detection delay by taking advantage of the AUV's two crossings of the layer, as depicted in Fig. 3. On the vehicle's first crossing on the ascent leg, the peak detection comes with a delay, but we let the vehicle save the past peak height in a sliding window. On the second crossing on the descent leg, as soon as the fluorescence measurement reaches the saved peak height (plus meeting additional timing and depth conditions that will be given in Section II-E), a sampling is triggered. The key components of the peak detection and triggering algorithm are elaborated upon in Sections II-A–II-E.

A. Tracking of Background Levels: Generating an Adaptive Threshold

First, a running average (from the start time to present) of the raw fluorescence measurements is calculated to provide the background level

$$\begin{aligned}\mathrm{FL}_{\mathrm{bkgd}}(n) &= \frac{1}{n+1}\sum_{i=0}^{n}\mathrm{FL}(i)\\ &= \frac{n\mathrm{FL}_{\mathrm{bkgd}}(n-1)+\mathrm{FL}(n)}{n+1}\end{aligned} \tag{1}$$

where i is the time index, n is the index of the current time, and $\mathrm{FL}(i)$ is the raw fluorescence measurement. The iterative formulation is used in the real-time computation.

Likewise, running averages of raw backscatter measurements are calculated to provide the background level (for both 470- and 676-nm wavelengths)

$$\begin{aligned}\mathrm{BB}_{\mathrm{bkgd}}(n) &= \frac{1}{n+1}\sum_{i=0}^{n}\mathrm{BB}(i)\\ &= \frac{n\mathrm{BB}_{\mathrm{bkgd}}(n-1)+\mathrm{BB}(n)}{n+1}\end{aligned} \tag{2}$$

where $\mathrm{BB}(i)$ is the raw backscatter measurement.

To reduce spurious peaks due to noise, the raw measurements are lowpass filtered by an M-sample moving-average window

$$\mathrm{FL}_{lp}(n) = \frac{1}{M}\sum_{i=0}^{M-1}\mathrm{FL}(n-i) \tag{3}$$

$$\mathrm{BB}_{lp}(n) = \frac{1}{M}\sum_{i=0}^{M-1}\mathrm{BB}(n-i). \tag{4}$$

Two operationally defined criteria for a thin phytoplankton layer are as follows[2]: 1) the peak fluorescence value exceeds twice the background level; and 2) the corresponding backscatter value also exceeds twice the background level. To avoid noise-induced peaks, we use the lowpass filtered signals $\mathrm{FL}_{lp}(n)$ and $\mathrm{BB}_{lp}(n)$ to check against the criteria. A detected peak of fluorescence qualifies as a "real peak" only when both criteria are met

$$\begin{aligned}&\text{If}\ \frac{\mathrm{FL}_{lp}(n)}{\mathrm{FL}_{\mathrm{bkgd}}(n)} \geq \alpha_{fl} \quad \text{AND} \quad \frac{\mathrm{BB}_{lp}(n)}{\mathrm{BB}_{\mathrm{bkgd}}(n)} \geq \alpha_{bb}\\ &\text{a "real peak" is detected}: \mathrm{FL\_PEAK}(i) = \mathrm{FL}_{lp}(n)\end{aligned} \tag{5}$$

where i is the peak index, and α_{fl} and α_{bb} are both set to 2 (note that the second criterion is for either of the two backscatter wavelengths). The thresholds for a "real peak" are thus adaptively adjusted in real time relative to the background.

B. Peak Detection by Slope Tracking

For fluorescence peak detection on the first crossing, we employ the basic approach of slope tracking. We define a state variable [15] S_{FL}, and two other variables $\mathrm{FL}_{\max}$ and $\mathrm{FL}_{\min}$ for storing the maximum and minimum fluorescence values. The definitions of the states are as follows:

$$\begin{aligned}&\text{If}\ \mathrm{FL}_{lp}(n) > \mathrm{FL}_{\max},\\ &\text{set}\ S_{\mathrm{FL}}(n)\ \text{to 1, and update}\ \mathrm{FL}_{\max}\ \text{by}\ \mathrm{FL}_{lp}(n).\\ &\text{If}\ \mathrm{FL}_{lp}(n) < \mathrm{FL}_{\min},\\ &\text{set}\ S_{\mathrm{FL}}(n)\ \text{to 0, and update}\ \mathrm{FL}_{\min}\ \text{by}\ \mathrm{FL}_{lp}(n).\end{aligned} \tag{6}$$

A fluorescence peak is detected when S_{FL} changes from 1 to 0 (i.e., the slope changes from being positive to being negative). To prevent false state changes due to noise, we set two low-value thresholds $\delta_{\mathrm{FL\_rise}}$ and $\delta_{\mathrm{FL\_drop}}$ (both are positive numbers). Only a rise/drop that exceeds the corresponding threshold is considered significant enough to qualify as a nontrivial rise/drop. State changes occur as follows:

$$\begin{aligned}&\text{If}\ S_{\mathrm{FL}}(n-1) = 1\ \text{AND}\\ &\quad [[\mathrm{FL}_{lp}(n) - \mathrm{FL}_{\max} < -\delta_{\mathrm{FL\_drop}}]\ \text{OR}\\ &\qquad [\mathrm{FL}_{lp}(n)\ \text{has dropped twice in a row}]],\\ &\text{flip}\ S_{\mathrm{FL}}(n)\ \text{to 0. A peak is detected.}\\ &\text{If}\ S_{\mathrm{FL}}(n-1) = 0\ \text{AND}\ \mathrm{FL}_{lp}(n) - \mathrm{FL}_{\min} > \delta_{\mathrm{FL\_rise}},\\ &\text{flip}\ S_{\mathrm{FL}}(n)\ \text{to 1.}\end{aligned} \tag{7}$$

The effect of $\delta_{\mathrm{FL\_rise}}$ is to prevent a small "bump" on a downslope (of fluorescence) from flipping S_{FL} from 0 to 1, while the effect of $\delta_{\mathrm{FL\_drop}}$ is to prevent a small "bump" on an upslope from flipping S_{FL} from 1 to 0 (i.e., detecting a peak).

We want the algorithm to be more sensitive to detecting a peak than to flipping from state 0 to state 1, so we set $\delta_{\mathrm{FL\_drop}}$ to a smaller value (i.e., a lower threshold) than $\delta_{\mathrm{FL\_rise}}$. See Section III for an example.

C. Tracking of Peaks' Baseline: When to Call a Detected Peak a "High Peak"?

Since the AUV is equipped with only ten gulpers, their triggerings should only occur on high fluorescence peaks. For this purpose, the running average of the detected fluorescence peaks is taken as the peaks' baseline

$$\begin{aligned}&\mathrm{FL\_PEAK}_{\mathrm{baseline}}(k)\\&=\frac{1}{k+1}\sum_{i=0}^{k}\mathrm{FL\_PEAK}(i)\\&=\frac{k\mathrm{FL\_PEAK}_{\mathrm{baseline}}(k-1)+\mathrm{FL\_PEAK}(k)}{k+1}\end{aligned}\tag{8}$$

where i is the peak index, $k+1$ is the number of detected peaks up to present, and $\mathrm{FL\_PEAK}(i)$ is the value of the detected peak. Only those peaks that are above $\mathrm{FL\_PEAK}_{\mathrm{baseline}}(k)$ qualify as "high peaks"

$$\text{If } \mathrm{FL\_PEAK}(k) > \mathrm{FL\_PEAK}_{\mathrm{baseline}}(k),\quad \text{consider } \mathrm{FL\_PEAK}(k) \text{ a "high peak".}\tag{9}$$

Thus, the threshold for a "high peak" is also adaptively adjusted in real time. Note that for the first peak $(k = 0)$, $\mathrm{FL\_PEAK}_{\mathrm{baseline}}(0) = \mathrm{FL\_PEAK}(0)$, so the above condition is not met, which disqualifies the first peak as a high peak. Only later peaks $(k \geq 1)$ can qualify as high peaks. This allows for some time for $\mathrm{FL\_PEAK}_{\mathrm{baseline}}$ to stabilize.

As illustrated in Fig. 3, presuming the fluorescence peak detected at the first crossing on the ascent leg exceeds the peaks' baseline $\mathrm{FL\_PEAK}_{\mathrm{baseline}}$, then at the second crossing on the descent leg, the vehicle is likely to encounter the peak again due to the thin layer's horizontal extent. As the two adjacent crossings are only separated by a short distance, the two peak measurements are likely to have similar heights. On the second crossing, when the fluorescence measurement reaches the saved peak height (saved on the first crossing), an AUV gulper is triggered. As a thin layer's intensity may vary over distance, the peak heights at the first and second crossings may have a small difference. If the second peak is lower than the first (i.e., the saved peak height), there will be no triggering. This actually serves our objective of triggering gulpers only on high peaks. Conversely, if the second peak is slightly higher than the first, the gulper will be triggered slightly before the second peak arrives. Since the water sample takes 1–2 s to fill the gulper, triggering slightly early will tend to center the sample on the peak.

D. Timing of the First-Peak Detection and the Subsequent Triggering: On an Ascent Leg or a Descent Leg?

The threshold for triggering at the second crossing is set by the peak height saved on the first crossing, based on the assumption of similar peak heights at the two consecutive crossings. Since horizontal variation in peak height is more probable with a larger horizontal separation, minimizing the separation between the pair of layer crossings is important. If the thin layer lies in the upper half of the yo-yo profile, the first-peak detection should occur on the ascent leg and the subsequent triggering should occur on the descent leg (as shown in the left panel in Fig. 4). Conversely, if the thin layer lies in the lower half of the yo-yo profile, the first-peak detection should occur on the descent leg and the subsequent triggering should occur on the ascent leg (as shown in the right panel in Fig. 4). Thus, the distance between the first-peak detection and the subsequent triggering is no more than half the distance spanned by one yo-yo cycle.

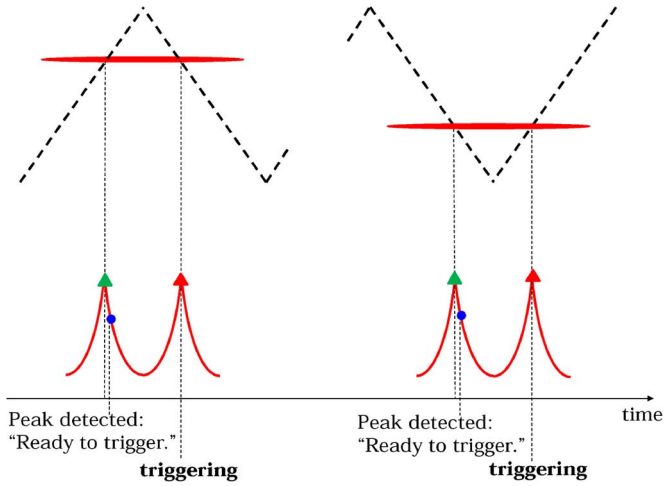

Fig. 4. The AUV determines the timing of the first-peak detection and the subsequent triggering based on whether the thin layer lies in the upper or lower half of the AUV's yo-yo profile.

Using the same algorithm as presented in Section II-B, the AUV tracks the state of its own depth by a variable S_{DEP} ($S_{\mathrm{DEP}} = 1$: descending; $S_{\mathrm{DEP}} = 0$: ascending), and tracks in real time the maximum and minimum depths by variables $\mathrm{DEP}_{\max}$ and $\mathrm{DEP}_{\min}$. The real-time middepth of the yo-yo pattern is $\mathrm{DEP}_{\mathrm{mid}} = (\mathrm{DEP}_{\max} + \mathrm{DEP}_{\min})/2$.

When a high fluorescence peak [satisfying the condition in (9)] is detected on the first crossing, the corresponding depth $\mathrm{DEP}(n)$ is compared with $\mathrm{DEP}_{\mathrm{mid}}$. Only if $S_{\mathrm{DEP}} = 1$ (i.e., the AUV is descending) plus $\mathrm{DEP}(n) > \mathrm{DEP}_{\mathrm{mid}}$ (i.e., the thin layer lies in the lower half of the yo-yo profile), or $S_{\mathrm{DEP}} = 0$ (i.e., the AUV is ascending) plus $\mathrm{DEP}(n) < \mathrm{DEP}_{\mathrm{mid}}$ (i.e., the thin layer lies in the upper half of the yo-yo profile), does the peak qualify as a "pretrigger peak" (preparing for a subsequent triggering on the second crossing).

E. Additional Conditions for Triggering a Sampling

For triggering a sampling, besides the condition of reaching a fluorescence peak, we also add the T_{lockout} and $\mathrm{DEP}_{\mathrm{lockout}}$ conditions just as in the threshold triggering method (introduced in Section I). Note that T_{lockout} is for the entire AUV mission, not for each yo-yo cycle.

III. Tests by the LOCO Experiment AUV Dataset

In the 2005 Layered Organization in the Coastal Ocean (LOCO) field program [2] in Monterey Bay, CA, a Dorado AUV conducted 20 surveys on a triangular track (as shown by the dashed lines in Fig. 5, counterclockwise starting from the

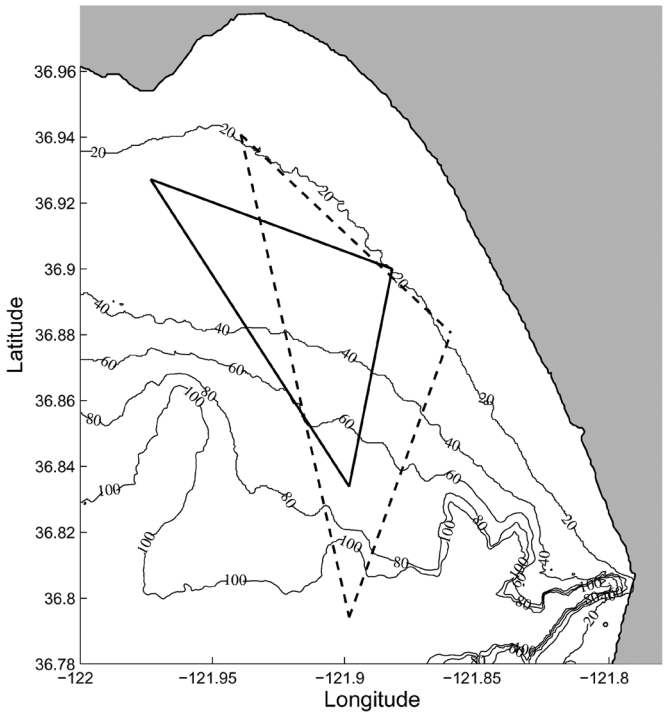

Fig. 5. The triangular survey tracks of the Dorado AUV in the 2005 LOCO Experiment (dashed line), and in the October 2009 AUV Mission 2009.280.00 (solid line). Labeled contours are bathymetry (in meters). Longitude: West. Latitude: North.

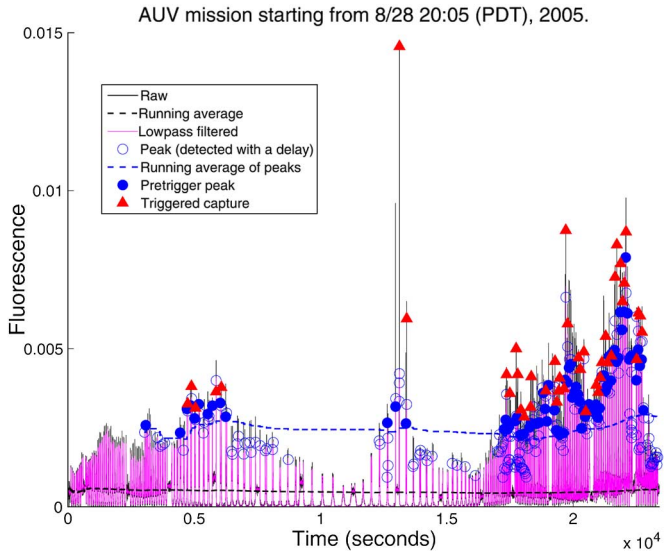

Fig. 6. Unconstrained peak-detection triggerings (red triangles) in postprocessing of the Dorado AUV Mission 2005.241.02 data.

northernmost vertex) from August 18 to September 6 [5]. The vehicle flew on a yo-yo trajectory in the vertical dimension, from 2.5-m depth down to 7 m above the bottom (the deepest point was about 100 m). The vehicle's horizontal and vertical speeds were about 1.5 and 0.5 m/s, respectively. The perimeter of the triangle was about 38 km. Taking into account that the AUV periodically ascended to surface for global positioning system (GPS) fixes, each one-lap survey took about 6.5 h. In this section, we test the adaptive peak-detection triggering method by postprocessing the full data set of the 20 AUV surveys. The algorithm is coded in MATLAB and runs on a desktop computer.

For example, we show the test result on AUV Mission 2005.241.02 (starting from 20:05:27 on August 28, 2005 (PDT), lasting for 6.5 h) in Fig. 6. The raw fluorescence measurement is shown by the black solid line. The background level, tracked by $\mathrm{FL}_{\mathrm{bkgd}}$ as calculated by (1), is shown by the black dashed line. Similarly, $\mathrm{BB}_{\mathrm{bkgd}}$ tracks the background level of backscatter on the 470- and 676-nm wavelengths. The lowpass filter (the same as the sliding window that saves the peak height on the first crossing) length M is set to 8 for calculating FL_{lp} and BB_{lp} by (3), (4). FL_{lp} is shown by the magenta line. α_{fl} and α_{bb} in (5) are both set to 2. To disqualify very small bumps as peaks, we set $\delta_{\mathrm{FL\_rise}}$ and $\delta_{\mathrm{FL\_drop}}$ in (7) to small nonzero values 10^{-4} and 10^{-5} (set empirically based on inspection of the FL_{lp} time series), respectively. $\delta_{\mathrm{FL\_drop}}$ is set to a lower value than $\delta_{\mathrm{FL\_rise}}$ as explained in Section II-B. As long as those two parameters are very small compared with the signal level, the performance of the peak-detection algorithm is not sensitive to their values, as will be shown at the end of this section.

In Fig. 6, the detected fluorescence peaks that exceed twice the background level (with the corresponding backscatter value also exceeding twice the background level) are shown by the blue circles. (Note that before 3000 s, backscatter values do not exceed twice the background level, hence there was no qualified fluorescence peak.) The average height of the fluorescence peaks, tracked by $\mathrm{FL\_PEAK}_{\mathrm{baseline}}$ as calculated by (8), is shown by the blue dashed line. The pretrigger peaks (as defined at the end of Section II-D) are marked by the blue filled circles. To fully reveal the triggerings' statistics, we do not exert the lockout time and lockout depth constraints (i.e., setting T_{lockout} and $\mathrm{DEP}_{\mathrm{lockout}}$ both to zero). There are 44 triggerings, as marked by the red triangles.

For performance comparison, we also test the threshold triggering method using the same data. We set $\mathrm{FL}_{\mathrm{thresh}}$ to a level, as previously applied in field tests of the threshold triggering method, specifically at the 80th percentile of all fluorescence measurements in the mission. In Fig. 7, for each triggering, we plot the fluorescence profiles on the first and the second crossings of the thin layer.

1) Using the threshold triggering algorithm, on the first crossing (blue), a triggering (blue triangle) occurs as soon as the preset $\mathrm{FL}_{\mathrm{thresh}}$ is reached. A triggering can occur well before the arrival of the actual peak (blue circle), thus missing the peak by a relatively large error.
2) Using the peak-detection algorithm, the actual peak on the first crossing is detected and saved in a sliding window to prepare for the triggering on the ensuing second crossing (red). On the second crossing, when the fluorescence measurement reaches the saved peak height on the first crossing, a triggering (red triangle) occurs. As discussed at the end of Section II-C, if the second peak (red circle) is slightly higher than the first (blue circle), the triggering will come slightly before the arrival of the second peak,

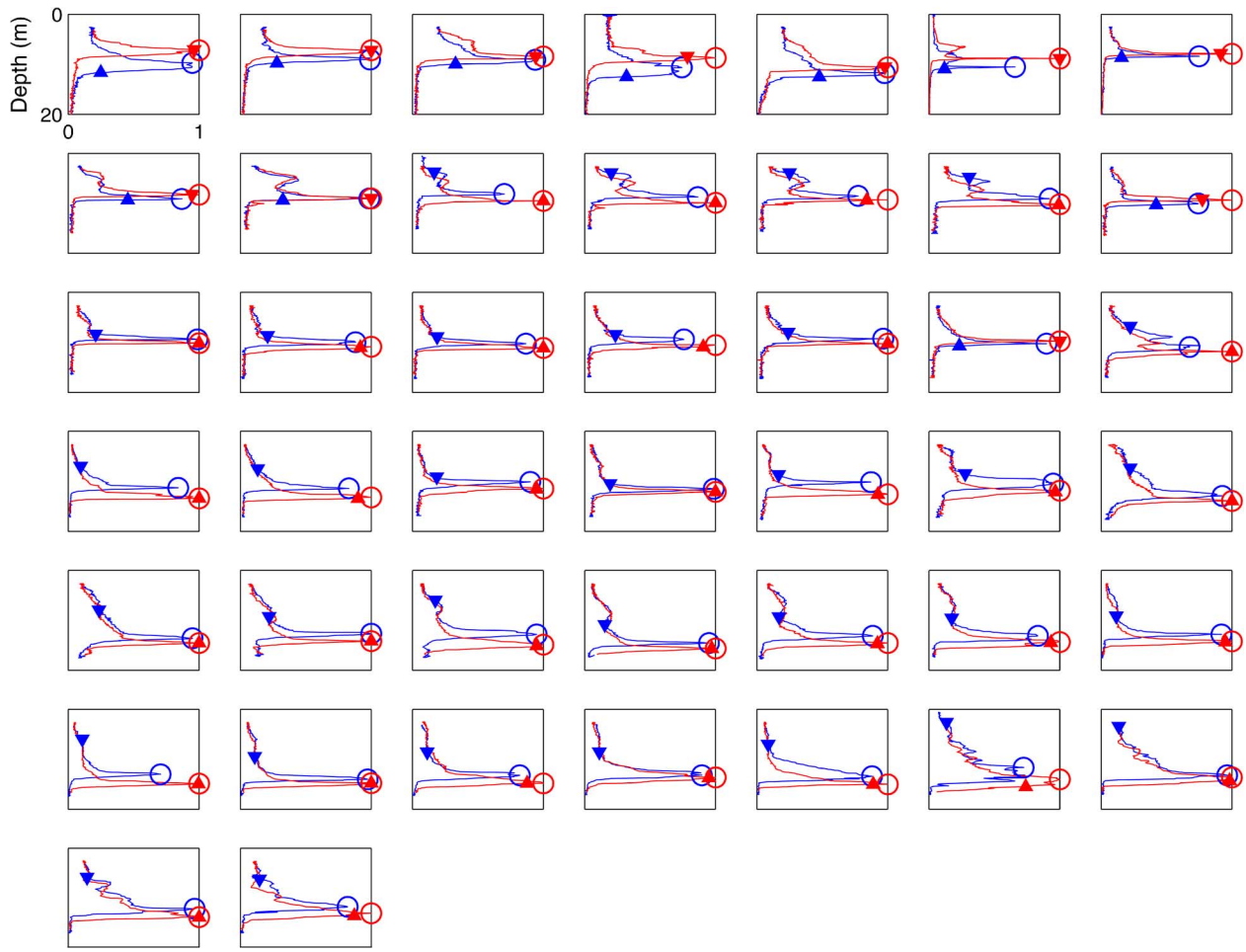

Fig. 7. Fluorescence profiles (normalized by the peak) for the triggerings in AUV Mission 2005.241.02. Blue: the first crossing of the thin layer. Red: the ensuing second crossing. Circle: the actual peak on each crossing. Blue triangle: the threshold triggering point. Red triangle: the peak-detection triggering point. The direction of the triangle indicates the AUV was ascending or descending.

but this error is typically small. Fig. 7 demonstrates that in most peak-detection triggerings, the triggering point overlaps or lies very close to the second peak. Note that the peak depths on the two crossings can have some difference if the thin layer is not level. This depth difference does not hinder the algorithm because the triggering on the second crossing depends on the value, rather than the depth, of the fluorescence peak on the first crossing.

Next, we test the two methods by the entire data set of the 20 AUV surveys, which produce about 310 peak-detection triggerings and as many threshold triggerings (for comparison purposes). To evaluate the peak-capture performance, we examine the following two errors, as shown in Fig. 8.

1) The triggering depth error $\mathrm{dep}_{\mathrm{err}} = \mathrm{depth}_{\mathrm{true\_peak}} - \mathrm{depth}_{\mathrm{triggering}}$, where $\mathrm{depth}_{\mathrm{true\_peak}}$ is the depth of the actual peak, and $\mathrm{depth}_{\mathrm{triggering}}$ is the depth of the triggering. The depth error by peak-detection triggering is very small (mean $= 0.08$ m and standard deviation $= 0.98$ m), much better than that by threshold triggering (mean $= -0.4$ m and standard deviation $= 3.6$ m). Also note that the peak-detection triggerings' depth errors are well centered around zero, while the threshold triggerings' depth errors have a bimodal distribution because a triggering almost always comes earlier than the actual peak (shallower than the actual peak if on a descent leg, or deeper than the actual peak if on an ascent leg).
2) The triggering level error $fl_{\mathrm{err}} = fl_{\mathrm{true\_peak}} - fl_{\mathrm{triggering}}$, where $fl_{\mathrm{true\_peak}}$ is the actual fluorescence peak level, and $fl_{\mathrm{triggering}}$ is the fluorescence level at the triggering. The peak-detection triggerings very accurately capture the peaks (mean of $fl_{\mathrm{err}} = 0.0002$ and standard deviation of $fl_{\mathrm{err}} = 0.0004$), an order of magnitude more accurate than the threshold triggerings (mean of $fl_{\mathrm{err}} = 0.002$ and standard deviation of $fl_{\mathrm{err}} = 0.001$).

Fig. 9 shows the fluorescence histograms of the peak-detection triggering cluster and the threshold triggering cluster in relation to the whole population. The lower end of the peak-detection triggering cluster lies at the 91st percentile of the whole population, another demonstration of the peak-capture performance of the presented method. In contrast, the lower end of the threshold triggering cluster lies at the 66th percentile of the whole population. Note that in each individual AUV survey, we set the threshold to the 80th percentile level, but the lower end of the entire cluster of threshold triggerings turns out to lie only at the 66th percentile of the whole data set of the 20 AUV surveys.

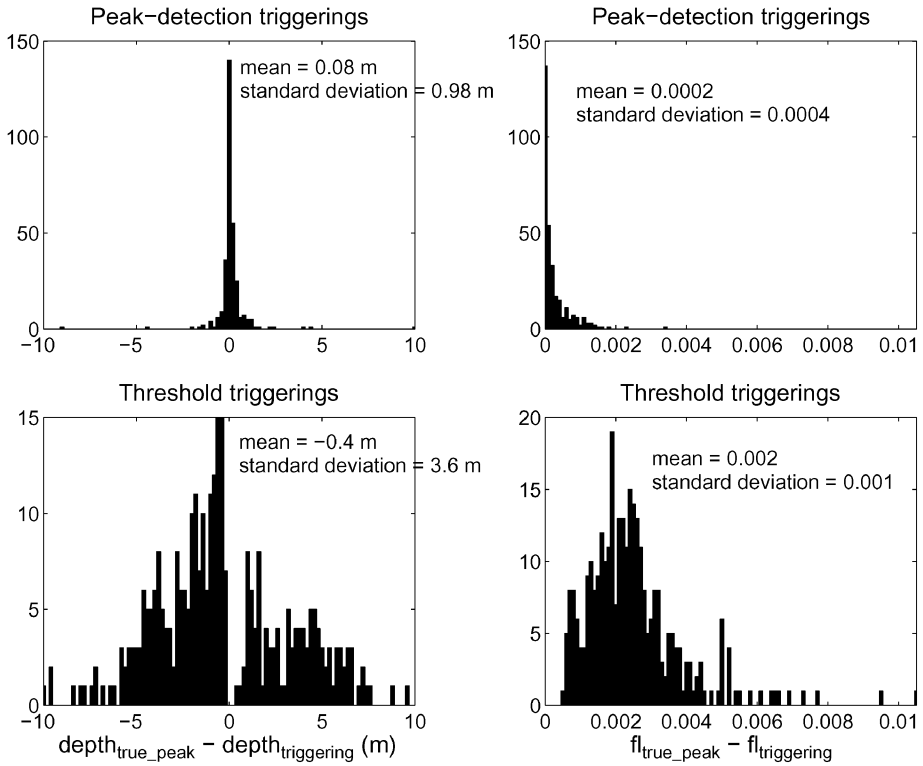

Fig. 8. Performance comparison of the two triggering methods on the entire data set of the 20 AUV surveys in the 2005 LOCO Experiment: the histograms of the triggering depth error (left) and the triggering level error (right).

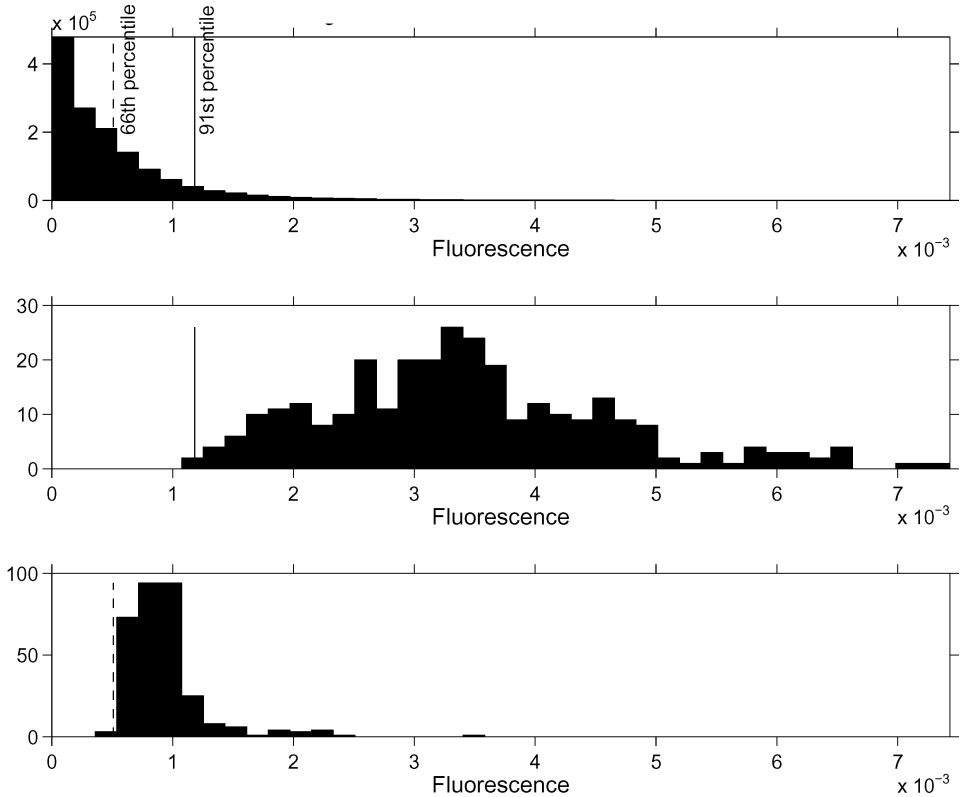

Fig. 9. The histograms of all fluorescence measurements in the 20 AUV surveys in the 2005 LOCO Experiment (upper panel), the fluorescence measurements at the peak-detection triggerings (middle panel), and those at the threshold triggerings (lower panel). The vertical dashed and solid lines mark the percentile of the lower end of the threshold triggering cluster and that of the peak-detection triggering cluster in the whole population, respectively.

To test the peak-detection algorithm's sensitivity to the values of $\delta_{\mathrm{FL\_rise}}$ and $\delta_{\mathrm{FL\_drop}}$, we compare the algorithm's performance at three different sets of $\delta_{\mathrm{FL\_rise}}$ and $\delta_{\mathrm{FL\_drop}}$ values for AUV Mission 2005.241.02, as shown in Table I. At higher values of $\delta_{\mathrm{FL\_rise}}$ and $\delta_{\mathrm{FL\_drop}}$, the total number of detected peaks drops because a larger number of small bumps are elimi-

TABLE I
PEAK-DETECTION ALGORITHM'S PERFORMANCE AT DIFFERENT VALUES OF $\delta_{\mathrm{FL\_rise}}$ AND $\delta_{\mathrm{FL\_drop}}$ FOR AUV MISSION 2005.241.02

δ_{FL_rise}, δ_{FL_drop}	Total number of detected peaks	Average height of detected peaks	Total number of triggerings	Average height of triggerings
0, 0	303	0.0027	44	0.005
10^{-4}, 10^{-5}	264	0.0028	44	0.005
2×10^{-4}, 2×10^{-5}	255	0.0029	44	0.0051

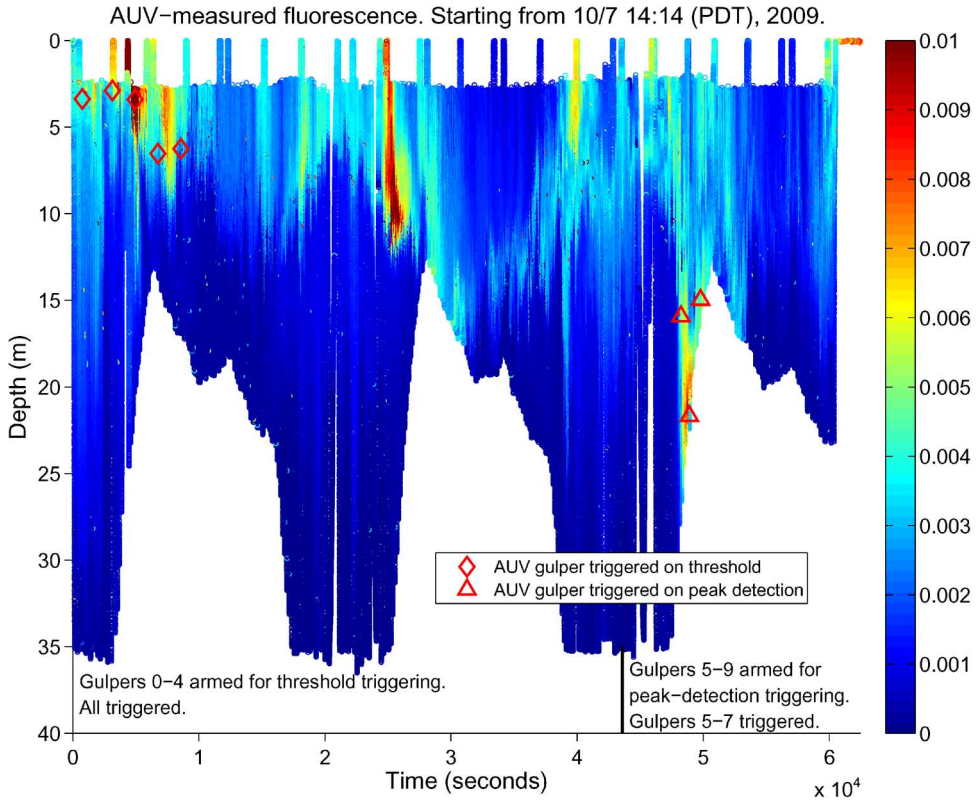

Fig. 10. During the Dorado AUV Mission 2009.280.00, the vehicle completed nearly three laps on the triangular track (as manifested by the repeated bathymetry). In the first lap, five gulpers were triggered on threshold. In the third lap, three gulpers were triggered on peak detection. Fluorescence measurement is the raw reading from the sensor.

nated. Correspondingly, the average height of the detected peaks rises but only slightly (note that the eliminated bumps can lie at a low or high signal level). As a result, the average height of the triggerings [which are required to exceed the peaks' baseline $\mathrm{FL\_PEAK}_{\mathrm{baseline}}(k)$] also rises but only slightly, while the total number of triggerings remain the same. This shows that while small nonzero $\delta_{\mathrm{FL\_rise}}$ and $\delta_{\mathrm{FL\_drop}}$ help prevent small bumps from being detected as peaks, the performance of the peak-detection triggerings is not sensitive to the values of $\delta_{\mathrm{FL\_rise}}$ and $\delta_{\mathrm{FL\_drop}}$.

IV. FIELD TEST

On October 7, 2009, we field tested the presented method in Dorado AUV Mission 2009.280.00 [starting from 14:14:05 (PDT), lasting for 17 h] in northern Monterey Bay, CA. The algorithm was coded in C++ and ran in real time on the AUV computer. The vehicle ran counterclockwise on the sides of a triangle (as shown by the solid lines in Fig. 5, starting from the southernmost vertex). The three vertices of the triangle were set to be the mooring sites of three environmental sampling processors (ESPs) [16], so that the water samples acquired by the AUV's gulpers could be compared with the *in situ* biological analyses by the ESPs. The vehicle flew on a yo-yo trajectory in the vertical dimension, from 2.5-m depth down to 10 m above the bottom (the maximum depth was set to 35 m for good horizontal resolution). The vehicle's horizontal and vertical speeds were about 1.3 and 0.3 m/s, respectively (thus the flight-path angle of the yo-yo track was about 13°). The perimeter of the triangle was about 28.5 km. Taking into account that the AUV periodically ascended to surface for GPS fixes, it took the vehicle about 6 h to complete one lap. In the 17-h mission, the vehicle completed nearly three laps.

The distance spanned by the longest yo-yo cycle was about $(35\ \mathrm{m}/\tan(13^\circ))\times 2 = 303$ m. The distance between a peak detection (on the AUV's first crossing of a thin layer) and the subsequent triggering (on the second crossing) is no more than half that distance, i.e., about 150 m. Studies in [5] showed that the horizontal scales of thin-layer patches in Monterey Bay, CA, range from <100 m to >10 km, with a median of 320 m. Thus,

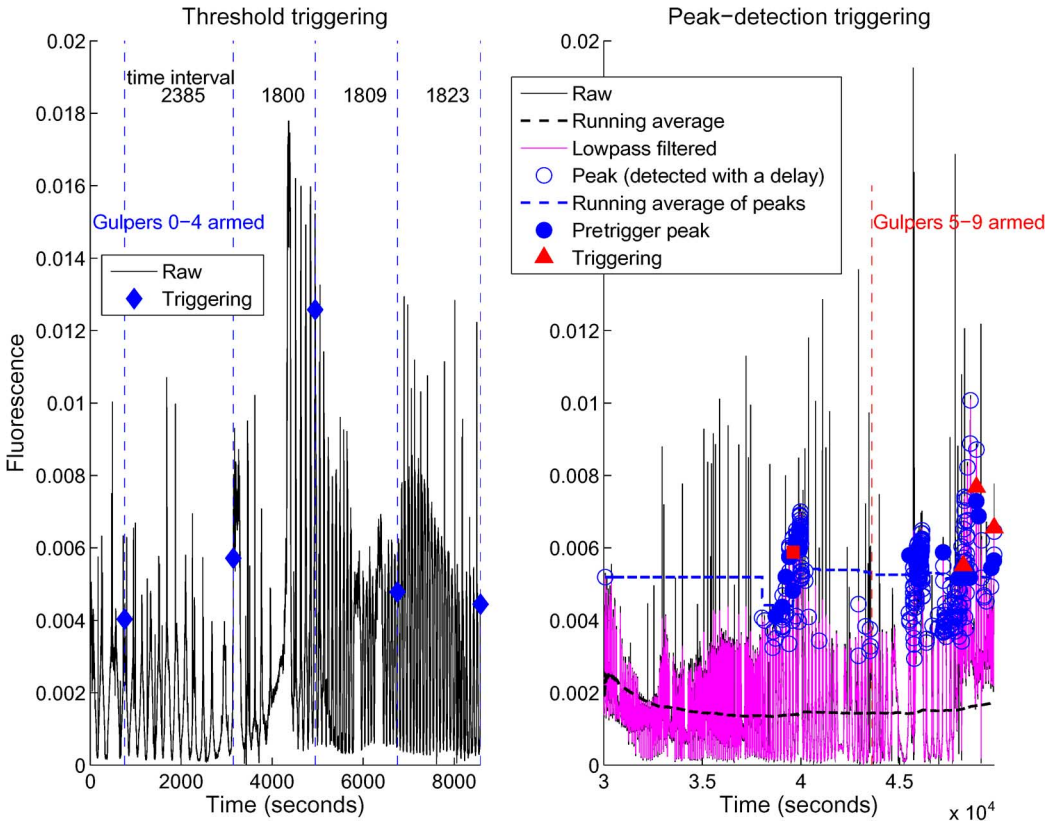

Fig. 11. The five threshold triggerings and the three peak-detection triggerings during the Dorado AUV Mission 2009.280.00.

our assumption of short distance between peak detection and triggering reasonably held.

During the AUV mission, we tested both the adaptive peak-detection triggering method and the threshold triggering method. We set five gulpers (numbers 0–4) to the threshold triggering mode, and set the other five gulpers (numbers 5–9) to the peak-detection triggering mode. In the AUV mission script, gulpers 0–4 were armed (i.e., enabled for triggering) at time zero (the start of the mission), and gulpers 5–9 were armed at time 43 599 s (when the AUV had finished the second lap on the triangular track). The gulpers' triggering modes and the actual triggerings are shown in Fig. 10.

A. Field Test Results of the Threshold Triggering Method

For threshold triggering, $\mathrm{DEP}_{\mathrm{lockout}}$ was set to 2 m, and T_{lockout} was set to 1800 s. K and J were set to 8 and 4, respectively (i.e., four out of eight past samples were required to exceed $\mathrm{FL}_{\mathrm{thresh}}$). By inspecting the fluorescence measurements in an AUV mission on the preceding day, we set $\mathrm{FL}_{\mathrm{thresh}}$ to 4×10^{-3}. In the early phase of the mission, gulpers 0–4 were all triggered to capture high-fluorescence water samples, as shown in the left panel in Fig. 11. This demonstrates that the threshold triggering method is a robust mechanism.

Near the second triggering, the fluorescence measurement rose sharply. As soon as four out of eight measurements exceeded $\mathrm{FL}_{\mathrm{thresh}}$, the second gulper was triggered (the fluorescence level at the triggering was about 6×10^{-3}). After that triggering, fluorescence continued to rise up to 8×10^{-3}, but threshold triggering was not designed to wait. After the second triggering, as soon as $T_{\mathrm{lockout}} = 1800$ s had elapsed, the AUV measured fluorescence exceeding $\mathrm{FL}_{\mathrm{thresh}}$ and the "J out of K" condition was also met, so the third gulper was immediately triggered. That triggering happened to fall on a "hot spot," capturing a very high fluorescence water sample.

B. Field Test Results of the Adaptive Peak-Detection Triggering Method

The peak-detection triggering algorithm was kicked off at 30 000 s (the middle of the mission), and gulpers 5–9 were armed at a later time at 43 599 s (the end of the second lap). The settings of $M, \alpha_{fl}, \alpha_{bb}, \delta_{\mathrm{FL\_rise}}$, and $\delta_{\mathrm{FL\_drop}}$ were the same as those used in Section III. Since triggerings were to occur only on high peaks, "dense triggerings" were less likely than using the threshold triggering method. Hence, we set T_{lockout} to a reduced value of 600 s. $\mathrm{DEP}_{\mathrm{lockout}}$ was still set to 2 m. Gulpers 5–7 were triggered, as shown in the right panel in Fig. 11. The red square marks a fluorescence peak that satisfied the triggering conditions but no triggering occurred because gulpers 5–9 were not armed yet.

Diurnal variation of the thin layer [5] is noted in Fig. 10: it migrated down from 5-m depth (for the triggerings of gulpers 0–4) to 20-m depth (for the triggerings of gulpers 5–7), while the fluorescence signal strength weakened. The details of the three peak-detection triggerings are given in Fig. 12 and described as follows.

1) Gulper 5: The AUV detected a fluorescence peak (the blue filled circle) on the ascent leg. The fluorescence level was higher than the peaks' baseline (the blue dashed line), thus was considered a high peak. Although the peak detection came with a delay, the true peak height (the green triangle) was saved in the sliding window (marked by the two vertical

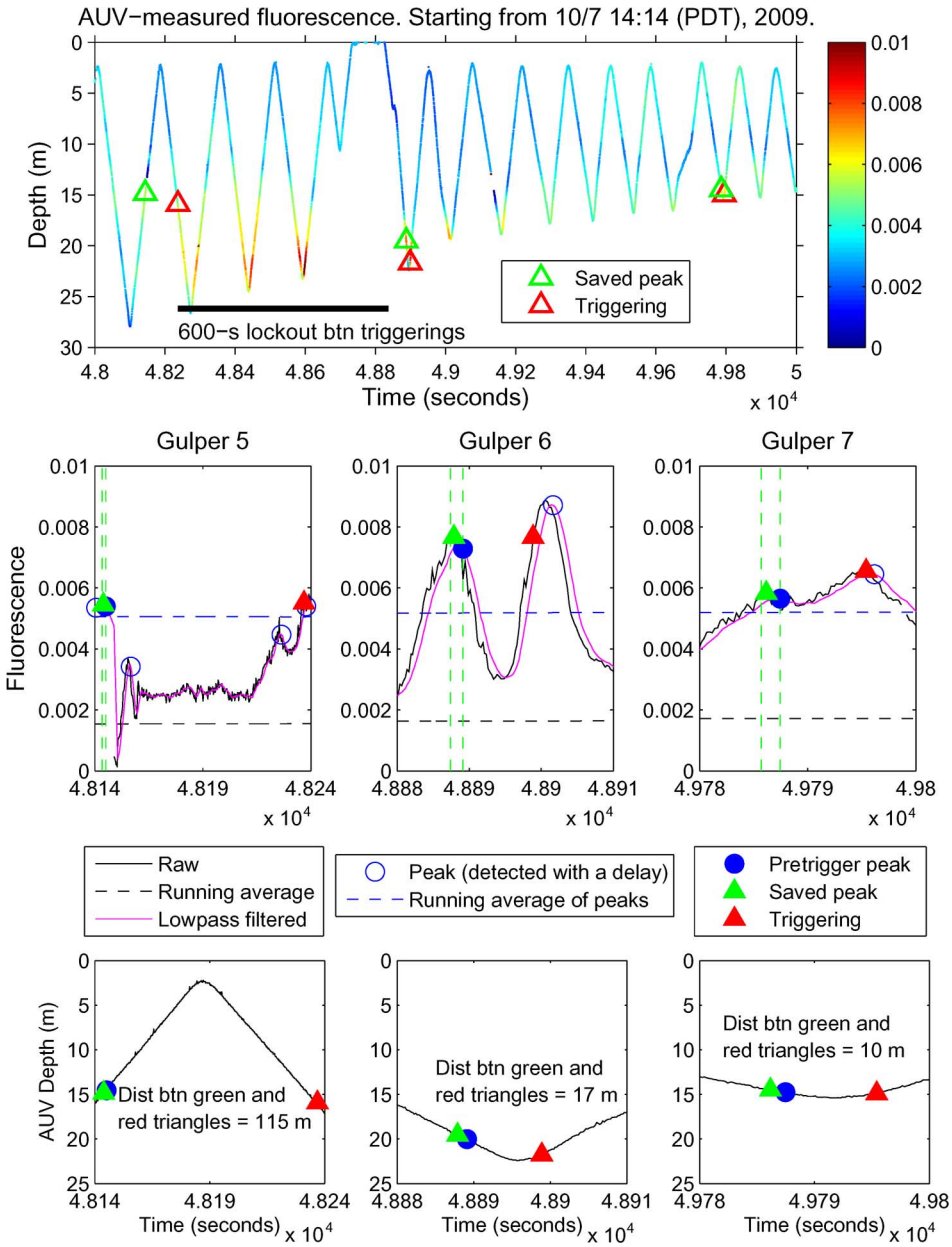

Fig. 12. Details of the peak-detection triggerings of gulpers 5, 6, and 7. In each middle panel, the two vertical dashed lines mark the sliding window that saved the true peak height on the first crossing of the thin layer. Fluorescence measurement is the raw reading from the sensor.

dashed lines). On the descent leg, as soon as the measured fluorescence exceeded the saved peak height, gulper 5 was triggered (the red triangle). When the fluorescence peak was detected on the ascent leg, the corresponding depth was shallower than $\mathrm{DEP}_{\mathrm{mid}}$ (see Section II-D). Hence, the vehicle determined that the thin layer lay in the upper half of the yo-yo profile, so the subsequent triggering occurred on the descent leg. Note that since the thin layer slanted downward, the triggering point (the red triangle) on the descent leg was slightly deeper than the pretrigger peak (the blue filled circle) on the ascent leg. The horizontal distance between the saved peak (on the ascent leg) and the triggering point (on the descent leg) was 115 m.

2) Gulper 6: The AUV detected (with a delay) a high fluorescence peak on the descent leg, and saved the true peak height in the sliding window. On the ascent leg, as soon as the measured fluorescence exceeded the saved peak height, gulper 6 was triggered. The horizontal distance between the saved peak and the triggering point was 17 m.
3) Gulper 7: The AUV detected (with a delay) a high fluorescence peak on the descent leg, and saved the true peak height in the sliding window. A triggering was to occur after the vehicle turned from descent to ascent. In our algorithm, the criterion for such an attitude change is that the vehicle has ascended at least 0.5 m from the turning point. When the vehicle had just ascended 0.5 m from the turning point, the measured fluorescence already exceeded the saved peak height, so gulper 7 was immediately triggered. That explains why the fluorescence level at the triggering was higher than the saved peak height. The horizontal distance between the saved peak and the triggering point was 10 m.

$$\mathrm{FL\_PEAK}_{\mathrm{baseline}}(k) = \begin{cases} \dfrac{1}{k+1}\sum_{i=0}^{k}\mathrm{FL\_PEAK}(i), & k < L_{\mathrm{window}} - 1 \\ \dfrac{1}{L_{\mathrm{window}}}\sum_{i=k-(L_{\mathrm{window}}-1)}^{k}\mathrm{FL\_PEAK}(i), & k \geq L_{\mathrm{window}} - 1 \end{cases} \tag{10}$$

A main advantage of the adaptive peak-detection triggering method is that there is no need to preset a triggering threshold. Instead, the thresholds (the background level $\mathrm{FL}_{\mathrm{bkgd}}$ and the peaks' baseline $\mathrm{FL\_PEAK}_{\mathrm{baseline}}$) are adaptively learned from real-time measurements. For the three peak-detection triggerings (gulpers 5–7), $\mathrm{FL\_PEAK}_{\mathrm{baseline}}$ turned out to be 5×10^{-3}. This automatically produced level was actually higher than the preset threshold $\mathrm{FL}_{\mathrm{thresh}} = 4\times10^{-3}$ for the five threshold triggerings. Note that the fluorescence signal strength had subsided (compared with the early phase of the mission) when gulpers 5–7 were triggered. Even so, the average height of the three peak-detection triggerings (0.0067) was not lower than that of the five threshold triggerings (0.0063).

For this AUV mission, $\mathrm{FL\_PEAK}_{\mathrm{baseline}}$ was calculated as the running average of the detected peaks from time zero (defined as when the peak-detection algorithm started to run) to present, as expressed in (8). A defect of this formula is: if the peaks are strong in the early stage of the AUV mission but become weaker in the later stage, the early strong peaks will set $\mathrm{FL\_PEAK}_{\mathrm{baseline}}$ to a high level. If the later peaks are lower than this level, they will miss the opportunity of being sampled. In this AUV mission, the fluorescence peak strength in the first half of the mission was significantly higher than that in the second half. Fortunately, since the peak-detection algorithm started only from the middle of the mission, the above problem was circumvented. A long-term solution is to calculate $\mathrm{FL\_PEAK}_{\mathrm{baseline}}$ in a sliding window instead from time zero. This way, $\mathrm{FL\_PEAK}_{\mathrm{baseline}}$ is only determined by the recent peaks. Posterior to the above AUV mission, we have revised the calculation of $\mathrm{FL\_PEAK}_{\mathrm{baseline}}$ from (8) to (10), shown at the top of the page, where i is the peak index, $\mathrm{FL\_PEAK}(i)$ is the value of the detected peak, and $k+1$ is the number of detected peaks up to present. L_{window} is the number of peaks within the sliding window, which is set based on how fast the peak strength may vary during an AUV mission. For example, in a succeeding AUV mission, we set the window length to 20 min.

V. Conclusion and Future Work

We have developed an adaptive triggering method for an AUV to capture water samples at chlorophyll fluorescence peaks in a thin phytoplankton layer. Tests by a previous data set of 20 AUV missions demonstrate the method's excellent performance in capturing peaks. In the October 2009 field test in northern Monterey Bay, CA, an MBARI Dorado AUV ran the algorithm in real time and successfully triggered three samplings at the peaks in a thin layer.

The tests have also revealed several aspects for improvement. The purpose of setting a minimum time interval T_{lockout} between triggerings is to prevent using up the gulpers over a short distance. If T_{lockout} is too small, the AUV may run out of gulpers too early, before more significant fluorescence signals show up. If T_{lockout} is too large, the AUV may miss significant fluorescence signals and end up with empty gulpers. For example, as shown in the upper panel in Fig. 12, strong fluorescence signals between the first and second triggerings did not trigger a gulper due to the 600-s lockout time. T_{lockout} should be adaptively adjusted instead of being fixed. Following the scheme in [17], T_{lockout} can be adjusted based on the number of triggerings so far and the signal level. If the detected fluorescence peak is high and the number of triggerings so far is low, T_{lockout} needs to be reduced to allow for more triggerings, expressed as follows:

$$\begin{aligned} &\text{If } \left[\left[\frac{\mathrm{FL\_PEAK}(k)}{\mathrm{FL\_PEAK}_{\mathrm{baseline}}(k)} > \beta\right] \text{ AND } \right. \\ &\qquad \left.\left[N_{\mathrm{gulpers\_triggered}} < N_{\mathrm{gulpers\_total}}\frac{T_{\mathrm{elapsed}}}{T_{\mathrm{whole\_mission}}}\right]\right], \\ &\text{reduce } T_{\mathrm{lockout}} \end{aligned} \tag{11}$$

where $N_{\mathrm{gulpers\_total}}$ and $N_{\mathrm{gulpers\_triggered}}$ are the total number of gulpers and the number of already-triggered gulpers so far, respectively. $T_{\mathrm{whole\_mission}}$ and T_{elapsed} are the whole mission duration and the elapsed time, respectively. $\beta > 1$ is some appropriate ratio.

An interesting feature to add is to let the AUV adaptively shrink the vertical range of its yo-yo profiles once a thin layer is detected, so that samplings can better concentrate on the thin layer. If the vertical range is narrow enough, the vehicle will closely track the layer. We previously developed a method for an AUV to track an internal tidal wave by way of closely following the thermocline. A new capability of tracking a thin layer will be very useful for coastal studies.

Acknowledgment

The authors would like to thank the MBARI Dorado AUV team H. Thomas, D. Thompson, and D. Conlin, as well as the *R/V Zephyr* crew. The authors appreciate the assistance and support from M. McCann, K. Gomes, and K. Headley, and the helpful comments from J. Harvey, R. Vrijenhoek, and C. Scholin. They would also like to thank the three anonymous reviewers for their valuable comments and suggestions for improving the paper.

References

[1] T. J. Cowles, R. A. Desiderio, and M.-E. Carr, "Small-scale planktonic structure: Persistence and trophic consequences," *Oceanography*, vol. 11, no. 1, pp. 4–9, 1998.

[2] J. M. Sullivan, M. A. McManus, O. M. Cheriton, K. J. Benoit-Bird, L. Goodman, Z. Wang, J. P. Ryan, M. Stacey, D. V. Holliday, C. Greenlaw, M. A. Moline, and M. McFarland, "Layered organization in the coastal ocean: An introduction to planktonic thin layers and the LOCO project," *Continental Shelf Res.*, vol. 30, no. 1, pp. 1–6, 2010.

[3] M. A. McManus, R. M. Kudela, M. W. Silver, G. F. Steward, P. L. Donaghay, and J. M. Sullivan, "Cryptic blooms: Are thin layers the missing connection?," *Estuaries Coasts*, vol. 31, pp. 396–401, 2008.

[4] J. P. Ryan, M. A. McManus, J. D. Paduan, and F. P. Chavez, "Phytoplankton thin layers caused by shear in frontal zones of a coastal upwelling system," *Mar. Ecol. Progr. Ser.*, vol. 354, pp. 21–34, 2008.
[5] J. P. Ryan, M. A. McManus, and J. M. Sullivan, "Interacting physical, chemical and biological forcing of phytoplankton thin-layer variability in Monterey Bay, California," *Continental Shelf Res.*, vol. 30, no. 1, pp. 7–16, 2010.
[6] J. G. Bellingham, K. Streitlien, J. Overland, S. Rajan, P. Stein, J. Stannard, W. Kirkwood, and D. Yoerger, "An arctic basin observational capability using AUVs," *Oceanography*, vol. 13, no. 2, pp. 64–71, 2000.
[7] D. R. Thompson, "AUV operations at MBARI," in *Proc. MTS/IEEE OCEANS Conf.*, Vancouver, BC, Canada, Oct. 2007, DOI; 10.1109/OCEANS.2007.4449212.
[8] MBARI, "Lowering the threshold for ocean access," Moss Landing, CA, Annu. Rep., 2005, pp. 9–12.
[9] L. E. Bird, A. Sherman, and J. Ryan, "Development of an active, large volume, discrete seawater sampler for autonomous underwater vehicles," in *Proc. MTS/IEEE OCEANS Conf.*, Vancouver, BC, Canada, Oct. 2007, DOI: 10.1109/OCEANS.2007.4449303.
[10] Y. Zhang, R. S. McEwen, J. P. Ryan, and J. G. Bellingham, "An adaptive triggering method for capturing peak samples in a thin phytoplankton layer by an autonomous underwater vehicle," in *Proc. MTS/IEEE OCEANS Conf.*, Biloxi, MS, Oct. 2009.
[11] G. Vivó-Truyols, J. R. Torres-Lapasió, A. M. van Nederkassel, Y. V. Heyden, and D. L. Massart, "Automatic program for peak detection and deconvolution of multi-overlapped chromatographic signals. Part I: Peak detection," *J. Chromatogr. A*, vol. 1096, pp. 133–145, 2005.
[12] H. L. Van Trees, *Detection, Estimation, and Modulation Theory, Part I*. New York: Wiley, 1968, ch. 4.
[13] V. P. Andreev, T. Rejtar, H.-S. Chen, E. V. Moskovets, A. R. Ivanov, and B. L. Karger, "A universal denoising and peak picking algorithm for LC-MS based on matched filtration in the chromatographic time domain," *Anal. Chem.*, vol. 75, pp. 6314–6326, 2003.
[14] P. Du, W. A. Kibbe, and S. M. Lin, "Improved peak detection in mass spectrum by incorporating continuous wavelet transform-based pattern matching," *Bioinformatics*, vol. 22, no. 17, pp. 2059–2065, 2006.
[15] V. T. Jordanov, D. L. Hall, and M. Kastner, "Digital peak detector with noise threshold," in *Proc. IEEE Nuclear Sci. Symp.*, Norfolk, VA, Nov. 2002, vol. 1, pp. 140–142.
[16] C. Scholin, G. Doucette, S. Jensen, B. Roman, D. Pargett, R. M. , III, C. Preston, W. Jones, J. Feldman, C. Everlove, A. Harris, N. Alvarado, E. Massion, J. Birch, D. Greenfield, R. Vrijenhoek, C. Mikulski, and K. Jones, "Remote detection of marine microbes, small invertebrates, harmful algae and biotoxins using the environmental sample processor (ESP)," *Oceanography*, vol. 22, pp. 158–167, 2008.
[17] Y. Zhang, J. G. Bellingham, and J. W. Bales, "Event triggering for AUV missions in the Labrador Sea experiment," MIT Sea Grant AUV Lab, Cambridge, MA, Tech. Rep., Nov. 1997.

Yanwu Zhang (S'95–M'00–SM'05) was born in 1969 in Shaanxi Province, China. He received the B.S. degree in electrical engineering and the M.S. degree in underwater acoustics engineering from Northwestern Polytechnic University, Xi'an, China, in 1989 and 1991, respectively, the M.S. degree in electrical engineering and computer science from the Massachusetts Institute of Technology (MIT), Cambridge, in 1998, and the Ph.D. degree in oceanographic engineering from the MIT/Woods Hole Oceanographic Institution (WHOI) Joint Program, Cambridge/Woods Hole, MA, in June 2000.

From 2000 to 2004, he was a Systems Engineer working on medical image processing at the General Electric Company (GE) Research and Development Center, Niskayuna, NY, and then a Senior Digital Signal Processing (DSP) Engineer at Aware Inc., Bedford, MA, working on digital communications. Since December 2004, he has been with the Monterey Bay Aquarium Research Institute, Moss Landing, CA, as a Senior Research Specialist. He works on developing and field-testing adaptive sampling algorithms for autonomous underwater vehicles (AUVs), designing sampling strategy for ocean observatories comprising AUVs and moorings, and developing a long-range AUV Tethys. His current research interests are mainly in spatio–temporal signal processing and its applications to AUV's sampling of oceanographic processes.

Dr. Zhang was a finalist for the MIT's *Technology Review Magazine* 100 young innovators (TR100) in 1999. He served as a reviewer for the IEEE JOURNAL OF OCEANIC ENGINEERING, the IEEE TRANSACTIONS ON NEURAL NETWORKS, *Journal of Atmospheric and Oceanic Technology*, *Journal of Geophysical Research (Oceans)*, *Deep-Sea Research*, *Ocean Engineering*, and *International Journal of Neural Systems*, as well as for the National Science Foundation (NSF) and the National Oceanic and Atmospheric Administration (NOAA) proposals. He was invited to chair sessions at the 2007 American Geophysical Union (AGU) Fall Meeting and the 2010 MTS/IEEE OCEANS Conference. He is a member of AGU and Sigma Xi.

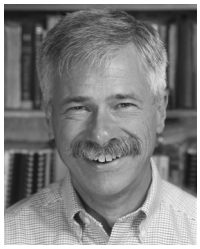

Robert S. McEwen (M'99) was born in Cleveland, OH, in 1955. He received the B.S. degree in electrical engineering from Purdue University, West Lafayette, IN, in 1978, the M.S. degree in electrical engineering from the University of Illinois, Chicago, in 1982, and the M.S. degree in mechanical engineering from Stanford University, Stanford, CA, in 1988. His specialization was dynamics and control.

He worked at Lockheed Corporation from 1982 to 1988 on spacecraft attitude control and navigation. From 1988 to 1997, he worked at Integrated Systems Incorporated on a variety of control-system related projects, from automotive power steering to spacecraft control. He was the Principal Engineer for the control system of the Miniature Sensor Technology Integration (MSTI) spacecraft, which operated successfully in orbit for over a year, exceeding its design life. Since 1998, he has worked primarily on autonomous underwater vehicle (AUV) guidance, navigation, and control systems for the Monterey Bay Aquarium Research Institute, Moss Landing, CA. Projects include a successful ocean AUV docking system, and more recently, GNC algorithms and simulations for a benthic imaging AUV that is constrained to fly at low (3 m) altitudes.

John P. Ryan was born in Lafayette, IN, in 1965. He received the B.S. degree in biology from the University of Massachusetts, Boston, in 1988 and the M.S. and Ph.D. degrees in biological oceanography from the University of Rhode Island, Narragansett, in 1993 and 1998, respectively.

He began a postdoctoral research position at the Monterey Bay Aquarium Research Institute (MBARI), Moss Landing, CA, in fall 1998, transitioned to MBARI Scientist in 2001, and is now Senior Research Specialist. His research integrates multidisciplinary observations from satellites, aircraft, ships, moorings, autonomous underwater vehicles (AUVs), and towed undulating vehicles to study ocean processes. In this research, he works extensively with engineers to advance AUV capabilities for marine science.

Dr. Ryan was awarded a fellowship by the Office of Naval Research in support of his M.S., and a NASA New Investigator Research grant in support of his postdoctoral research.

James G. Bellingham received the B.S./M.S. degrees in physics and the Ph.D. degree in physics from the Massachusetts Institute of Technology (MIT), Cambridge, in 1984 and 1988, respectively.

He is the Chief Technologist at the Monterey Bay Aquarium Research Institute (MBARI), Moss Landing, CA. His personal research activity revolves around the development and use of autonomous underwater vehicles (AUVs). He leads the Autonomous Ocean Sampling Network (AOSN) program at MBARI, which uses fleets of autonomous vehicles to adaptively observe dynamic oceanographic processes. He has spent considerable time at sea, leading over 20 AUV expeditions in environments ranging from the waters off Antarctica to the central Arctic. Before joining MBARI, he was at MIT, where he founded the Autonomous Underwater Vehicle Laboratory and ran it from 1988 to 2000. In 1997, he cofounded Bluefin Robotics Corporation, a leading manufacturer of AUVs.

Dr. Bellingham received the Lockheed Martin Award for Ocean Science and Engineering from the Marine Technology Society. He serves on a number of advisory boards and councils, including the Naval Research Advisory Committee and the Strategic Advisory Group for Battelle's National Security Division.